

# Polyelectrolyte Complexes of Chitosan and Poly(acrylic acid) As Proton Exchange Membranes for Fuel Cells<sup>†</sup>

B. Smitha, S. Sridhar, and A. A. Khan\*

Membrane Separations Group, Chemical Engineering Division,  
Indian Institute of Chemical Technology, Hyderabad-500 007, India

Received October 22, 2003; Revised Manuscript Received December 23, 2003

**ABSTRACT:** Ionically cross-linked polyelectrolyte complex (PEC) membranes of cationic chitosan (CS) and anionic poly(acrylic acid) (PAAc) were synthesized and assessed for applicability in fuel cells. CS and PAAc were blended in different weight ratios and the resulting membranes were posttreated to enable the formation of the polyelectrolyte complex. The ionic cross-linking occurring on blending the polyelectrolytes excludes the need of using other cross-linking agents. These membranes were extensively characterized for morphology, their intermolecular interactions, thermal stability, and physicochemical properties using SEM, FTIR, DSC, sorption studies, and tensile testing, respectively. Methanol permeability and proton conductivity were estimated and compared with respective values for Nafion 117. PEC membranes exhibited high ion exchange capacity (IEC), high proton conductivity, low methanol permeability, and adequate thermal and mechanical stability. Among the blends synthesized, the membrane blend with 50 wt % of CS and 50 wt % of PAAc, was identified as ideal for direct methanol fuel cell (DMFC) applications as it exhibited low methanol permeability ( $3.9 \times 10^{-8}$  cm<sup>2</sup>/s), excellent physicochemical properties and comparatively high proton conductivity (0.038 S·cm<sup>-1</sup>). Above all, the cost-effectiveness and simple fabrication technique involved in the synthesis of such PECs makes their applicability in DMFC quite attractive.

## Introduction

Fuel cell technology has been considered a promising alternative for future energy needs combined with cleaner environment.<sup>1–3</sup> Among the several kinds of fuel cells, the proton-exchange membrane fuel cell (PEMFC) and the direct methanol fuel cell (DMFC) are known to utilize proton conducting polymer membranes. However, the development of the PEM fuel cell has been sluggish due to the investment required for fabricating a suitable proton conducting polymer membrane that is stable at fuel cell operating conditions.<sup>4</sup> Owing to diverse energy demands, direct methanol fuel cell (DMFC), operating with liquid methanol directly as a fuel feed, has been attractive as an alternative power source.<sup>5</sup>

The configuration of DMFC is almost similar to that of PEMFC, except for the fuel and catalyst. Despite its relatively lower performance, DMFC is considered superior to PEMFC because of its simple fuel handling system and improved safety. Despite those advantages, there are several obstacles preventing the commercialization of DMFC, such as high cost, poor chemical, and thermal stability, reduced conductivity of the membranes, and most significantly the so-called “methanol crossover”, i.e., methanol diffusion from anode to cathode side across the polymer electrolyte membrane. The methanol crossover not only wastes fuel but also causes performance losses at the cathode due to the consumption of oxygen and catalyst poisoning.<sup>6,7</sup>

In recent years, there has been an intensive research effort to develop new membranes for DMFC applications.<sup>8–22</sup> The membrane in direct methanol fuel cells should not only conduct protons but also serve as a barrier for methanol; i.e., membranes have to fulfill the requirements both as effective proton conductors as well

as methanol barriers. In addition to this, water uptake of membranes should be reasonably low.

So far only a few types of membranes have been used for proton conduction in DMFC. Among them are perfluorinated ionomer Nafion,<sup>23</sup> polybenzimidazole/phosphoric acid blend membranes,<sup>8</sup> Nafion membranes modified with inorganic phase-like silicate<sup>10</sup> or zirconium phosphate<sup>16</sup> and acid–base membranes.<sup>24</sup> The disadvantages of the Nafion membranes are their high price and high methanol permeability. Recent literature describes the modifications suggested for Nafion membrane in a bid to improve its performance. The approaches described are diverse, ranging from treatment with phosphoric acid,<sup>8</sup> doping with inorganic ions,<sup>9</sup> and formation of Nafion-based organic/inorganic composites<sup>25</sup> to the in situ polymerization of imbedded polymer precursors,<sup>26</sup> which has proven to be expensive.

Mixing of negatively and positively charged polyelectrolytes leads to the formation of a complex by electrostatic interaction, and usually causes a precipitate or coacervate<sup>27</sup> in an aqueous medium. Such a compact precipitate, in the form of thin continuous film, has been developed<sup>28</sup> and applied to membrane separation processes such as dialysis, ultrafiltration, and reverse osmosis early in the 1960s,<sup>29</sup> and such polyelectrolyte complex membranes have been successfully used in the dehydration of alcohols.<sup>30</sup>

To date, polyelectrolyte complexes have not been investigated as candidates for proton-conducting membranes. In this study, polyelectrolyte membranes were prepared from different ratios of chitosan and PAAc. Anionic polyelectrolyte PAAc is known to possess high charge density based on the dissociated carboxyl group, and cationic polyelectrolyte chitosan is basic in nature and possess unique properties because of the presence of both amino and hydroxyl groups. The objective of this study is to investigate the applicability of this blend for a DMFC by estimating the methanol permeability, proton conductivity, and water uptake of the blend and

\* Corresponding author. E-mail: aakhan@iict.ap.nic.in. Telephone: 040-27193139; Fax: 040-27193626.

<sup>†</sup> IICT Communication No. 031208.

**Table 1. Typical Sample Preparation and Designation of Polyelectrolyte Membranes for Fuel Cell Applications**

designation	weight ratio chitosan/PAAc
PEC90/10	90/10
PEC80/20	80/20
PEC70/30	70/30
PEC60/40	60/40
PEC50/50	50/50
PEC25/75	25/75

to elucidate interactions between chitosan and PAAc using FTIR, thermal analysis and mechanical testing.

## Experimental Section

**Materials.** PAAc of molecular weight 450 000 and chitosan having a viscosity average molecular weight of 500 000 were purchased from Aldrich Chemical Co. The degree of N-deacetylation of chitosan was determined and found to be 86%. Formic acid was purchased from Loba Chemie, Mumbai, India.

**Membrane Preparation.** Solutions of PAAc (1 wt %) and chitosan (1 wt %) in 3.5 wt % aqueous formic acid were mixed in different proportions as listed in Table 1. The sample was designated PEC(chitosan wt %)/(PAAc wt %). For example, PEC80/20 represents the membrane containing 80 wt % chitosan and 20 wt % poly(acrylic acid). The solutions were cast on a clean glass plate and dried at 30 °C in a convection oven over 24 h. The membranes were then washed with water for 24–30 h to form a complex of PAAc and chitosan. Scheme 1 depicts these posttreatments carried out to render these blends water insoluble. Scheme 2 shows the formation of the polyelectrolyte complex with the ionic interactions and hydrogen bonding.

**SEM Studies.** The films were thoroughly dried, and the surface morphology was studied by scanning electron microscopy (SEM) using a Hitachi S2150 microscope. The SEM images for the polyelectrolyte blend PEC50/50 are shown in Figure 1.

**FTIR Studies.** The FTIR spectra of polyelectrolyte membranes, PAAc, and chitosan were scanned using Nicolet-740 and Perkin-Elmer-283B FTIR spectrometers. These spectra are shown in Figures 2 and 3.

**Thermal Analysis. DSC.** The DSC spectra of the polyelectrolyte and their blends were obtained on Perkin-Elmer DSC model 7. Measurements were performed over the temperature range of 30–200 °C at a heating rate of 5 °C/min in hermetically sealed aluminum pans. Membrane samples were allowed to attain steady state with the solvents and the sample pan was conditioned in the instrument before running the experiment. Results are shown in Figure 4.

**Determination of the Ion Exchange Capacity, Water and Methanol Uptake, and Mechanical Strength.** Ion exchange capacity (IEC) indicates the number of milliequivalents of ions in 1 g of the dry polymer. To determine the ion exchange capacity, specimens of similar weight were soaked in 50 mL of 0.01 N sodium hydroxide solution for 12 h at ambient temperature. Then, 10 mL of sample was titrated with 0.01 N sulfuric acid.<sup>31</sup> The sample was regenerated with 1 M hydrochloric acid, washed free of acid with water, and dried to a constant weight. The IEC was calculated according to the equation

$$\text{IEC} = \frac{B - P \times 0.01 \times 5}{m}$$

where IEC = ion exchange capacity (in mequiv/g),  $B$  = amount of sulfuric acid used to neutralize blank sample in mL,  $P$  = amount of sulfuric acid used to neutralize the polyelectrolyte membranes used in the study in mL, 0.01 = normality of the sulfuric acid, 5 = the factor corresponding to the ratio of the amount of NaOH taken to dissolve the polymer to the amount used for titration, and  $m$  = sample mass in g.

To determine the polymer–liquid interaction, preweighed samples of circular pieces of the polymer films (3 cm diameter)

were soaked in deionized water/methanol. The films were taken out after different soaking periods and quickly weighed after carefully wiping out excess water/methanol to estimate the amount absorbed at the particular time “ $t$ ”. The film was then quickly placed back in the solvent. The process was repeated until the films attained steady state as indicated by constant weight after a certain period of soaking time. The percentage sorption was calculated from the following equation:

$$\text{water uptake [\%]} = \frac{M_s - M_d}{M_d} \times 100$$

Here  $M_s$  = mass of the swollen polymer in g and  $M_d$  = mass of the dry polymer in g.

The equipment used for carrying out the test was a universal testing machine (UTM), model AGS-10kNG, made by Shimadzu with an operating head load of 5 kN. The cross-sectional area of the sample of known width and thickness was calculated. The films were then placed between the grips of the testing machine. The grip length was 5 cm and the speed of testing was set at the rate of 12.5 mm/min. Tensile strength was calculated using the equation

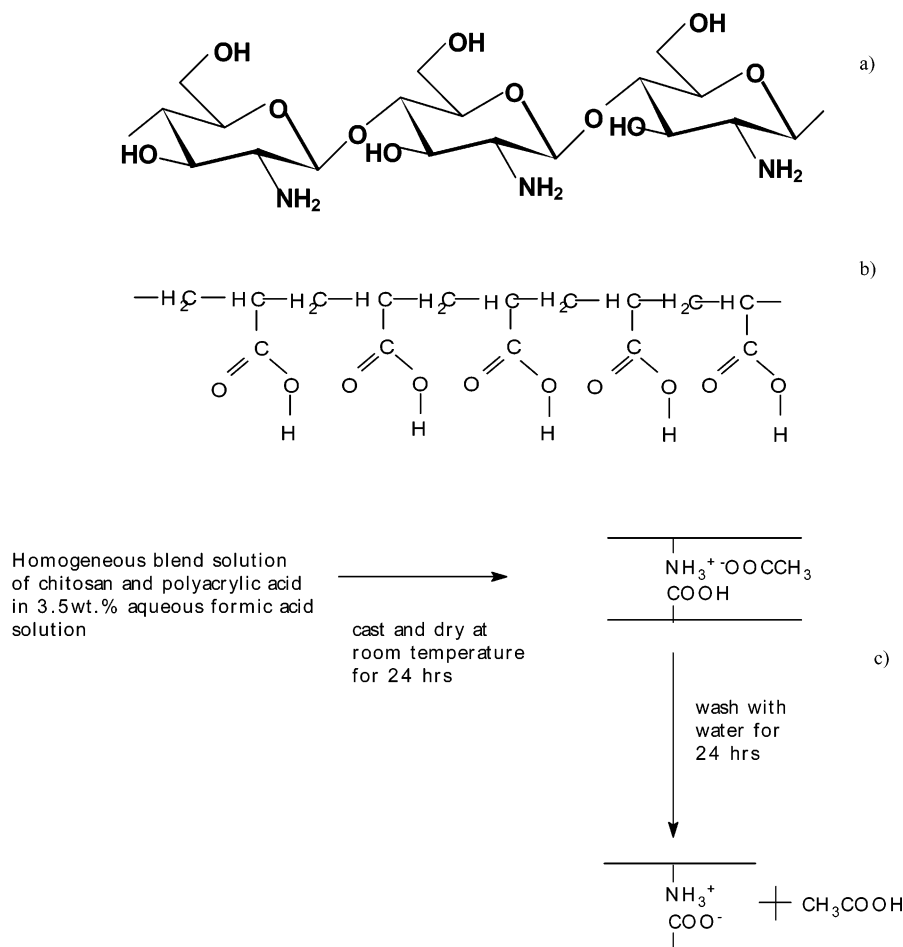
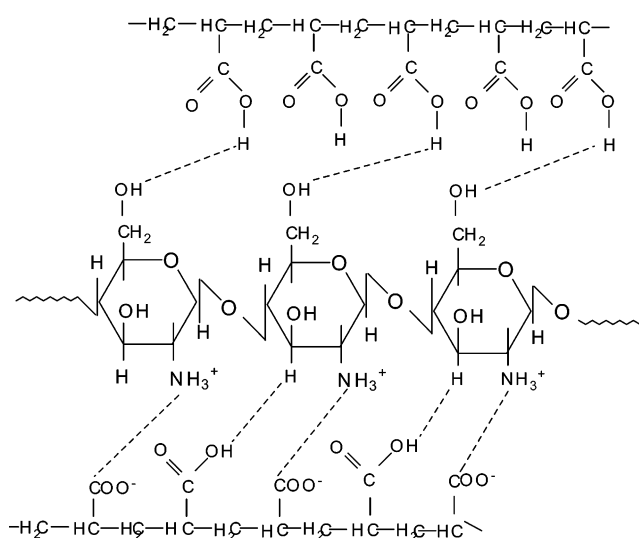
$$\text{tensile strength} = \frac{\text{maximum load}}{\text{cross-sectional area}} \text{ N/mm}^2$$

**Permeability.** Methanol permeability of the polyelectrolyte films was determined and calculated by the method described by Pivovar et al.<sup>32</sup> Prior to testing, membranes were hydrated in deionized water for at least 24 h. The concentration of methanol in permeate samples was determined by using gas chromatography (GC). Samples were analyzed using a Nucon 5765 gas chromatograph fitted with a DEGS packed column. A view of the cell used for methanol permeability is shown in Figure 5.

**Conductivity Measurements.** The proton conductivity in water-equilibrated membranes was determined by a four-electrode electrochemical impedance spectroscopy (EIS) method<sup>33,34</sup> using a PGSTAT20 frequency analyzer by EcoChemie B. V. Spectra and were recorded between 1 MHz and 0.1 Hz with 10 points per decade at a maximum perturbation amplitude of 10 mV. The impedance spectra were fitted on the basis of the equivalent circuit shown by Haufe et al.<sup>35</sup> The Zview 2.1b software by Scribner Associates Inc. was used for curve fitting procedure. To measure the temperature dependence of the conductivity, the cell was placed in a sealed, tempered, double-walled vessel and the temperature recorded in close proximity to the membrane with a K-type thermocouple. To avoid changes in the humidification levels during the measurements, a Teflon bowl filled with water was placed at the bottom of the vessel. Measurements were carried out in a conductivity cell at temperatures ranging from 30 to 150 °C. Figure 6 gives the schematic view of the conductivity cell.

## Results and Discussion

Scheme 1 represents the structures of the polymers synthesized for the study and also a schematic representation of the membrane formation. Scheme 2 shows the ionic interactions occurring on blending the two polyelectrolytes, which include (i) ionic cross-linking between ammonium ion ( $\text{NH}_3^+$ ) of CS and carboxylate ion ( $\text{COO}^-$ ) of PAAc, (ii) hydrogen bonding between  $\text{H}^+$  of carboxylic group of PAAc and  $\text{OH}^-$  of CS, and (iii) hydrogen bonding between  $\text{H}^+$  of CS and  $\text{OH}^-$  of carboxylic group of PAAc. These ionic interactions are confirmed by FTIR. All the three bonds exhibit affinity toward water and repel organic molecules such as methanol ( $\text{CH}_3\text{OH}$ ), thereby enabling hydration of the polymer matrix, which is essential for proton mobility. The ionic bond between  $\text{NH}_3^+$  and  $\text{COO}^-$  is the strongest one formed, which induces cross-linking and prevents

**Scheme 1. Structures of Chitosan (a) and Poly(acrylic acid) (b) and Schematic Description of Membrane Preparation (c)****Scheme 2. Formation of Polyelectrolyte Complex with Ionic Interactions and Hydrogen Bonding**

dissolution and excessive swelling of the polymer matrix in the presence of water.

Both the homopolymer and the blend solutions of PAAc and CS were optically clear to the naked eye. No separation into two layers or precipitation was observed when the membranes were allowed to stand for 1 month at room temperature. This can be demonstrated from the SEM pictures.

The solubility behavior of the polyelectrolyte complex membranes is shown in Table 2. It can be noticed that as the blending ratio approaches unity, the blend membranes remain insoluble in dilute formic acid. Further, the polyelectrolyte complex is insoluble in organic solvents indicating substantial chemical inertness.

**SEM.** Parts a and b of Figure 1 show the surface and cross-sectional views of the homogeneous complex blend membranes of chitosan and poly(acrylic acid). From both views, no phase separation of the membrane surface can be observed, suggesting that the synthesized polymeric blends are homogeneous and hence form dense membranes. This homogeneity of the blend film confirms the ionic interaction (that includes ionic cross-linking and hydrogen bonding) occurring on blending the two polymers. The surface of the polyelectrolyte complex shows no visible pores even at magnification up to  $100000\times$ , whereas the formation of few pores in the cross-sectional view is evidenced. This pore formation may be due to the miscible nature of aqueous formic acid (solvent for the polyelectrolyte complex) with water vapor in air. The membrane thickness estimated from the photomicrograph is  $30\ \mu\text{m}$ .

**FTIR Analysis.** FTIR spectra pertaining to the polyelectrolyte complex membranes prepared by blending chitosan and PAAc in various ratios is presented in Figure 2. It can be seen that the characteristic peaks of chitosan, viz., the hydroxyl and amide I and II groups, are located at  $3450\ \text{cm}^{-1}$  and  $1650, 1550\ \text{cm}^{-1}$  respec-



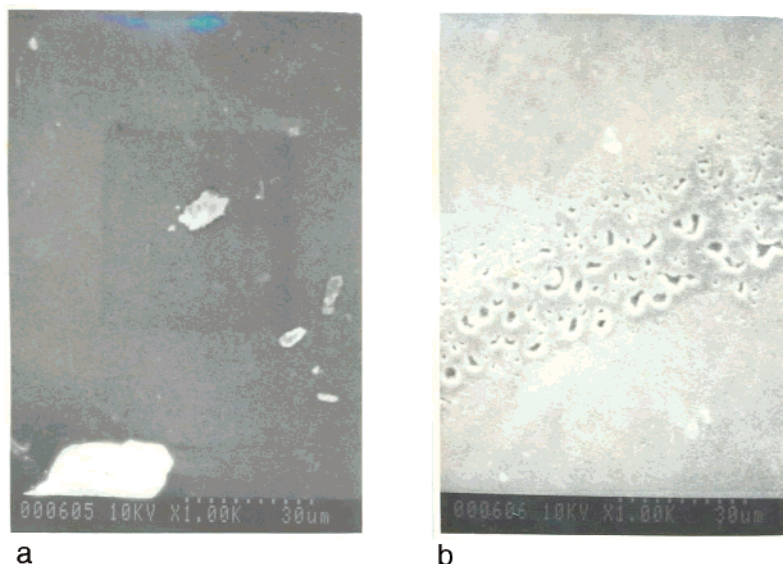


**Figure 1.** SEM picture of homogeneous polyelectrolyte complex membrane based on chitosan and poly(acrylic acid): (a) surface; (b) cross-section.

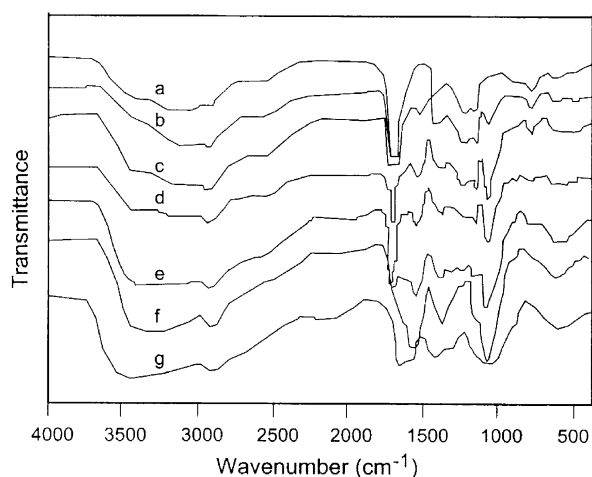


**Figure 2.** FTIR spectra of polyelectrolytes and their blends: (a) PAAc; (b) PEC2080; (c) PEC4060; (d) PEC5050; (e) PEC6040; (f) PEC8020; (g) CS.

tively. The FTIR spectrum of PAAc shows peaks around 3410, 1720, and 1450  $\text{cm}^{-1}$ . As the ratio of PAAc to chitosan increases, the characteristic C=O peak of PAAc appears (Figure 3). Formation of a new peak at 1550  $\text{cm}^{-1}$  in the spectra of the blend membranes can be evidenced. This may be assigned to the symmetric  $-\text{NH}_3^+$  deformation resulting on blending the two polymers. Broad peaks appearing at 2500 and 1900  $\text{cm}^{-1}$  in the blend membranes also confirm the presence of  $-\text{NH}_3^+$  as in chitosan. The negatively charged carboxylate ion ( $-\text{COO}^-$ ) and positively charged  $-\text{NH}_3^+$  coexist in the chitosan–PAAc complex membrane. Thus, the results of FTIR analysis clearly prove the formation of the polyelectrolyte complex of the acid–base blend.

**DSC.** The values of the glass transition temperature  $T_g$  of the polyelectrolytes and their blends were determined by the DSC technique at a heating rate of 10  $^\circ\text{C}/\text{min}$ . From Figure 4, it can be seen that chitosan shows a glass transition temperature of 170  $^\circ\text{C}$ , while PAAc exhibits a transition at 70  $^\circ\text{C}$ . Upon blending the polyelectrolytes, the  $T_g$  of chitosan reduced from 170 to 150  $^\circ\text{C}$  for PEC80/20, and that of PAAc shifted from 70 to 90  $^\circ\text{C}$  for PEC25/75. However, the transition of all the blends ranged between 70 and 170  $^\circ\text{C}$ .

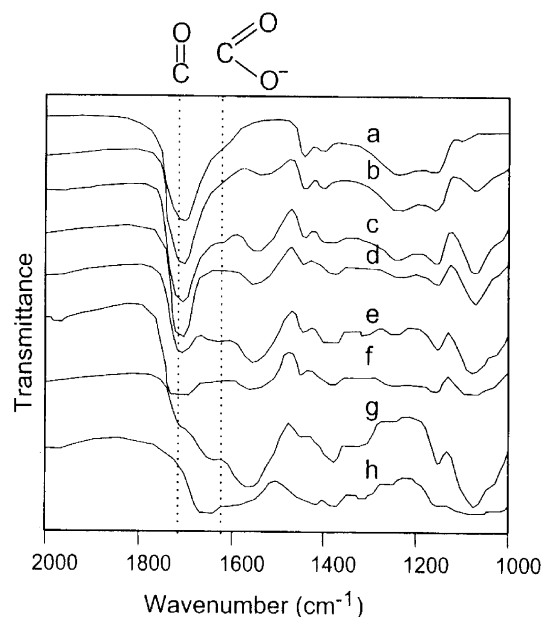


**Figure 3.** Characteristic FTIR spectra of poly(acrylic acid)–chitosan complex formation: (a) PAAc; (b) PEC2080; (c) PEC4060; (d) PEC5050; (e) PEC6040; (f) PEC7030; (g) PEC8020; (h) CS.

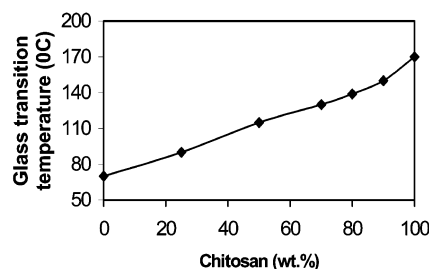


**Figure 4.**  $T_g$  of polyelectrolytes and their complexes as a function of wt % of chitosan.

This shift in the glass transition temperature can be attributed to the hydrogen bonding and ionic cross-linking occurring on blending the polyelectrolytes. Chitosan and PAAc in polyelectrolyte complexes have cationic ( $\text{NH}_3^+$ ) and anionic ( $\text{COO}^-$ ) groups, respectively,

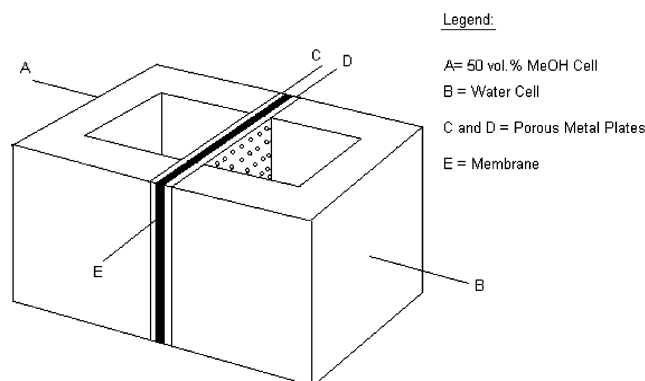


Figure 5. Methanol permeability cell.

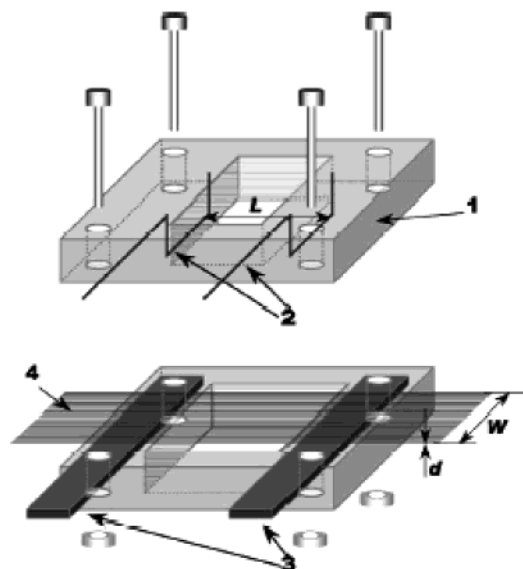


Figure 6. Four-point-probe conductivity cell for measuring ionic conductivities in membranes. Cell dimensions are approximately 3 cm  $\times$  3 cm  $\times$  1.4 cm: (1) Teflon block; (2) Pt wires for potential readout; (3) Pt foils for constant current supply; (4) membrane specimen (4 cm  $\times$  1 cm).

Table 2. Solubility Behaviors of the Polyelectrolyte Complex Membranes<sup>a</sup>

membrane	3.5 wt % aqueous formic acid	deionized water	NMP	DMSO	DMAc
PEC25/75	+ -	#	-	-	-
PEC50/50	-	-	-	-	-
PEC60/40	-	-	-	-	-
PEC70/30	-	-	-	-	-
PEC80/20	+ -	#	-	-	-
PEC90/10	+ -	#	-	-	-

<sup>a</sup> Key: (+ -) partially soluble; (-), insoluble; (#) exhibits swelling; (NMP) -n, methyl 2-pyrrolidone; (DMSO) dimethyl sulfoxide; (DMAc) dimethyl acetamide.

which can interact with each other, resulting in the shift in the glass transition temperature.

**IEC, Water and Methanol Uptake, and Mechanical Properties.** Ion exchange capacity (IEC) provides an indication of the ion exchangeable groups present in a polymer matrix, which are responsible for the conduction of protons and thus is an indirect and reliable approximation of the proton conductivity. Results are based on the sample calculations reported in Appendix 1. The IEC values of all the membranes used in the study are tabulated in Table 3. It can be seen that the IEC value ranged from 1.24 mequiv/g for

Table 3. IEC, Methanol Permeability, and Proton Conductivity of the Blend Membranes

membrane	ion exchange capacity (mequiv/g)	methanol permeability <sup>b</sup> ( $\times 10^{-8}$ cm <sup>2</sup> /s)	proton conductivity <sup>a</sup> ( $\times 10^{-2}$ S $\cdot$ cm <sup>-1</sup> )
PAAc	0.86		0.011
PEC25/75	1.24	4.8	0.030
PEC50/50	1.06	3.9	0.038
PEC60/40	1.18	4.1	0.035
PEC70/30	1.22	4.6	0.031
PEC80/20	1.16	8.2	0.027
PEC90/10	0.94	8.7	0.021
CS	0.91	-	0.031
nafion 117	0.91	27.6	0.086

<sup>a</sup> Conductivity measured at room temperature using 4-probe conductivity cell. <sup>b</sup> Measurements carried out at 30  $^{\circ}$ C, using 50% v/v methanol.

Table 4. Thickness, Sorption Characteristics, and Mechanical Strength of Blend Membranes<sup>a</sup>

membrane	thickness ( $\mu$ m)	% water uptake	% methanol uptake	tensile strength (MPa)	% elongation at break
PAAc	35	<i>b</i>	0.08	8.7816	8
PEC25/75	32	54	0.63	21.8122	7.3
PEC50/50	30	26	1.06	26.1045	4
PEC60/40	34	35	1.20	24.1084	5
PEC70/30	28	42	1.28	23.9137	7
PEC80/20	28	80	1.29	22.8071	7.5
PEC90/10	36	139	1.41	20.2856	8
CS	50	<i>c</i>	0.39	18.0673	4

<sup>a</sup> All the measurements were carried out at a temperature of 30–40  $^{\circ}$ C. <sup>b</sup> Completely soluble in water; hence, we could not measure. <sup>c</sup> Highly swollen in water, not measurable.

PEC25/75 to 0.94 mequiv/g for PEC90/10. PEC70/30 exhibited the highest ion exchange capacity of 1.22 mequiv/g.

Table 4 shows the equilibrium percentage sorption of water and methanol obtained by soaking the plain and blended membranes in the respective solvents at 30  $^{\circ}$ C. The stability of the membrane was analyzed by bending the membrane just before weighing the dried sample. The membrane is considered stable if its mechanical strength is restored after bending it (i.e., it does not break upon bending). All the blend membranes exhibited stability compared to CS and PAAc. Among the PEC blends, PEC50/50, PEC60/40, and PEC70/30 exhibited good stability as their mechanical properties were maintained. PEC25/75, PEC90/10, and PEC80/20 were somewhat brittle. PEC50/50 exhibited the least water sorption at 26%, followed by PEC60/40 at 35% and PEC70/30 at 42%. It can be observed that an increase in the PAAc content in the polyelectrolyte complex membranes, the closer is the packing of the chitosan chains because of the interlocking created by the PAAc, resulting in lower absorption. The methanol sorption of the blend membranes was quite low and ranged from 0.63% for PEC25/75 to 1.41% for PEC90/10.

The tensile strength at break of the blend membranes in dry state are given in Table 4. From the results, it can be observed that an increase in the chitosan concentration in the blend membrane causes an increase in the tensile strength and a reduction in the elongation at break of the blend membranes. This enhancement

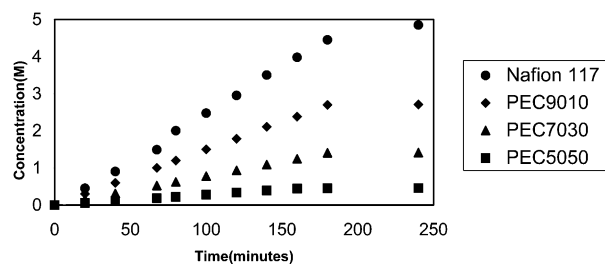


**Figure 7.** Typical diffusion data. The methanol aqueous solution concentration was 50 vol %. The slope of these lines is proportional to the methanol permeability.

may be attributed to the ionic-cross-linking of the polyelectrolyte membranes. Polymer chains in the polyelectrolyte complex having electrostatic interactions with another polymer chain experience a restriction in the mobility due to ionic-cross-linking. This restriction results in an increase in the rigidity or the tensile strength, thereby reducing the elongation at break.

**Methanol Permeability.** The values of methanol permeability for the test membranes are shown in Table 3. The notable feature is the permeability of Nafion 117 ( $27.6 \times 10^{-8} \text{ cm}^2/\text{s}$ ), which is three to four times higher than that observed in this work. This shows that a significant reduction in methanol crossover could be achieved by using membranes, which are much less permeable to methanol. It is known that the methanol permeability in Nafion increases with increasing methanol concentration,<sup>32</sup> but for the polyelectrolyte blends, used in this study, the trend is entirely reversed. From Figure 7, it can be observed that methanol permeability in Nafion increases with increasing concentration of methanol. Thus, at higher methanol concentrations, Nafion acts as a poor barrier, whereas the polyelectrolyte membranes exhibit good barrier properties.

Among the blends synthesized in this study, the polyelectrolyte blends PEC50/50, PEC60/40, and PEC70/30 showed relatively low methanol permeability. PEC50/50 displayed the lowest permeability of  $3.9 \times 10^{-8} \text{ cm}^2/\text{s}$ , followed by PEC60/40 ( $4.1 \times 10^{-8} \text{ cm}^2/\text{s}$ ) and PEC70/30 ( $4.6 \times 10^{-8} \text{ cm}^2/\text{s}$ ). This result can be explained on the basis of the lack of significant chemical interaction between methanol and the ionic clusters introduced on blending the polyelectrolytes. Ionized groups hydrate strongly and exclude organic solvents (salting-out effect), which is an essential feature for polymer electrolyte membranes.

**Proton Conductivity.** Measurement of conductivity is important to assess the contribution of various ionic groups in the blends. Table 3 provides a comparison of the conductivity of membranes synthesized in the study with that of Nafion 117 at room temperature. The polyelectrolyte blends exhibit higher conductivities compared to the anionic and cationic polyelectrolytes. The PEC50/50 blend showed better conductivity ( $0.038 \text{ S}\cdot\text{cm}^{-1}$ ) followed by the PEC60/40 ( $0.035 \text{ S}\cdot\text{cm}^{-1}$ ) and PEC70/30 ( $0.031 \text{ S}\cdot\text{cm}^{-1}$ ) blends. The values are approximately half of those obtained for Nafion 117 ( $0.086 \text{ S}\cdot\text{cm}^{-1}$ ). The high proton conductivity can be attributed to the hydroxyl and amine groups present in the polyelectrolytes, which give rise to hydrophilic regions in the polymer because of their strong affinity toward water. These hydrophilic areas formed around the cluster of side chains lead to absorption of water, enabling easy proton transfer.<sup>36</sup> The formation of hydronium ion ( $\text{H}_3\text{O}^+$ ) occurs when the fuel, ionized at the

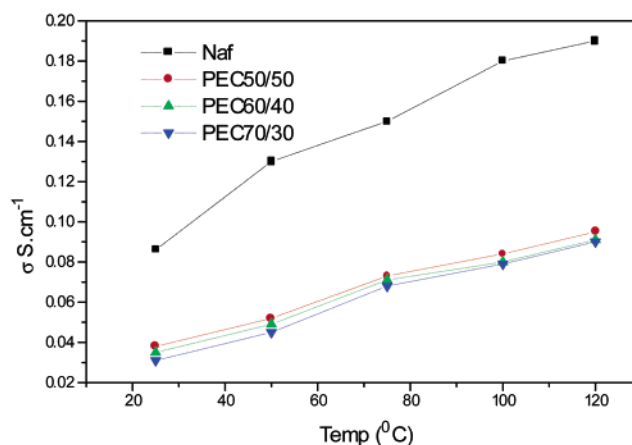


**Figure 8.** Proton conductivity vs temperature.

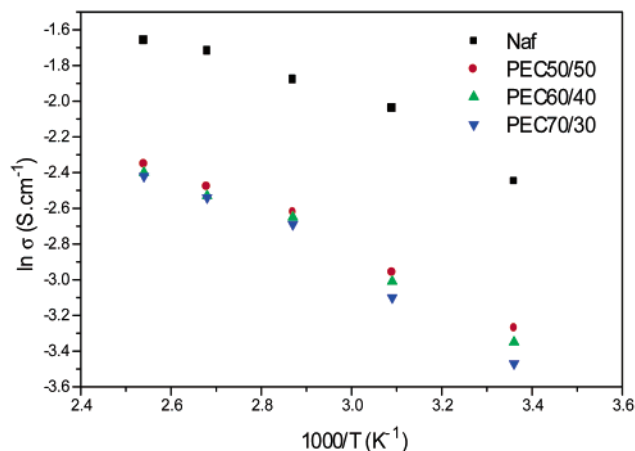


**Figure 9.** Arrhenius plot of conductivity vs temperature.

catalyst-coated anode, comes in contact with the water molecules. These hydronium ions pass through the hydrophilic regions of the membrane, releasing protons at the cathode.

The reduction in water absorption and swelling of the acid–base polyelectrolyte blends suggests that the acid groups are in close proximity, which may also contribute to an increase in the conductivity by ionic-cross-linking. Figure 8 represents the conductivity curve of polyelectrolyte blends as a function of temperature in the range 30–140 °C.

The Arrhenius plot in Figure 9 is an indication of the mechanism of proton transport. From the plot, the activation energy can be calculated, which shows that the proton transport might have occurred by two mechanisms. The first of these, is a Grotthuss or “jump” mechanism, which can be idealized as the proton being passed down the chain of water molecules. The second transport mechanism, called a vehicle mechanism, assumes a proton combines with the solvent molecules, yielding a complex like  $\text{H}_3\text{O}^+$ . This complex then diffuses intact. In Nafion, both mechanisms are believed to exist.

The activation energies for the synthesized polyelectrolyte complexes PEC50/50, PEC60/40, and PEC70/30 were found to be 13.4, 13.7, and 14.1  $\text{kJ}\cdot\text{mol}^{-1}$  respectively. In the Nafion membrane, the proton migration is primarily by the Grotthuss mechanism. In this mechanism, the proton which forms as  $\text{H}_3\text{O}^+$  ion jumps to the neighboring lone pair of electrons of a water molecule. For such a mechanism, the activation energy



for proton conduction should be around 14–40 kJ·mol<sup>-1</sup> and the values obtained for the polymers synthesized in this work, are close to the above values. Hence, it can be concluded from the Arrhenius plot that the proton transport might have occurred by both the mechanisms and predominantly by the vehicular mechanism.

## Conclusions

Polyelectrolyte complex membranes were prepared from chitosan and poly(acrylic acid) by mixing the respective polymer solutions in different weight ratios. FTIR characterization confirmed the ionic cross-linking resulting on blending the two polymers.

Characterization by DSC and tensile testing revealed adequate thermal and mechanical stability of the membranes which is essential for fuel cell applications. Moderate water sorption (20–40%) of the blends ensured high proton conductivity with no significant effect on mechanical stability. Though these membranes offer no significant advantages over Nafion, so far as proton conductivity is considered, the lower permeability to methanol when compared to Nafion renders them applicable to direct methanol fuel cells.

Among the blends synthesized in this study, PEC50/50 appears more suitable for fuel cell application considering its optimum physicochemical properties, thermal properties, methanol permeability, and proton conductivity. The technique of blending anionic and cationic polyelectrolytes results in membranes with properties better than the individual polyelectrolytes. The study thus reveals the possibility of preparing low cost acid–base polyelectrolyte blend membranes having IEC values comparable to that of Nafion but relatively lower methanol permeabilities. This result implies that an improvement in fuel utilization efficiency could be realized using polyelectrolyte complex membranes that control the magnitude of fuel by-pass.

**Acknowledgment.** The authors would like to thank Council of Scientific and Industrial Research, India for funding the Fuel Cell Project (ES/P 81-1-03, EMR Head). The help and support of Prof. Suryanarayana and colleagues of Physics Department in carrying out conductivity measurements is acknowledged. Help rendered by Mr. Kranthi Kiran, Membrane Separations Lab, Mr. Sai Babu, of the Design Section, Mr. Murari Lal, instrumentation for FTIR analysis, and Dr. M. Shakuntala, SEM analysis is gratefully acknowledged.

## Appendix 1: Calculations of IEC<sup>31</sup>

Consider the case of Polyelectrolyte blend membrane PEC90/10. Initial conditions: mass of dry PEC = 0.143 g; normality of H<sub>2</sub>SO<sub>4</sub> = 0.01 N (N<sub>1</sub>); normality of NaOH = 0.01 N (N<sub>2</sub>).

After 12 h: blank titer value = 10 mL; sample titer value = 7.3 mL; volume of NaOH neutralized = 10 mL.

The ion exchange capacity of the membrane is calculated as follows:

$$\begin{aligned} \text{IEC} &= \frac{(\text{blank titration} - \text{sample titration}) \times \text{normality} \times 5}{\text{membrane weight}} \\ &= \frac{(10 - 7.3) \times 0.01 \times 5}{0.1429} \\ &= 0.94 \text{ mequiv/g} \end{aligned}$$

IEC values for other ratios of the polyelectrolyte complex membranes were calculated along the same lines.

## References and Notes

- (1) Kordesch, K.; Simader, G. *Fuel Cells and their Applications*; VCH: Weinheim, Germany, 1996.
- (2) Cleghorn, C.; Ren, X.; Springer, T. E.; Wilson, M. S.; Zawodzinski, C.; Zawodzinski, T. A.; Gottesfeld, S. *Int. J. Hydrogen Energy* **1997**, *22*, 1137.
- (3) Ren, X.; Zelency, P.; Thomas, S.; Davey, J.; Gottesfeld, S. *J. Power Sources* **2000**, *86*, 111.
- (4) Hikita, S.; Yamane, K.; Nakajima, Y. *Soc. Autom. Eng. Jpn.* **2001**, *22*, 151.
- (5) Surampudi, S.; Narayanan, S. R.; Vamos, E.; Frank, H.; Halpert, G.; LaConti, A.; Kosek, J.; Prakash, G.; Olah, G. A. *J. Power Sources* **1994**, *47*, 377.
- (6) Ravikumar, M. K.; Shukla, A. K. *J. Electrochem. Soc.* **1996**, *143*, 2601.
- (7) Cruickshank, J.; Scott, K. *J. Power Sources* **1998**, *70*, 40.
- (8) Wainright, J. S.; Wang, J. T.; Weng, D.; Savinell, R. F.; Litt, M. H. *J. Electrochem. Soc.* **1995**, *142*, 121.
- (9) Tricoli, V. *J. Electrochem. Soc.* **1998**, *145*, 3798.
- (10) Arico, A. S.; Creti, P.; Antonucci, P. L.; Antonucci, V. *Electrochem. Solid-State Lett.* **1998**, *1*, 66.
- (11) Walker, M.; Baumgartner, K.-M.; Kaiser, M.; Ullrich, A.; Kellers, J.; Rauchle, E. *J. Appl. Polym. Sci.* **1999**, *74*, 67.
- (12) Carretta, N.; Tricoli, V.; Picchioni, F. *J. Membr. Sci.* **2000**, *166*, 189.
- (13) Kellers, J.; Ullrich, A.; Haring, Th.; Preidel, W.; Baldauf, M.; Gebhardt, U. *J. New Mater. Electrochem. Syst.* **2000**, *3*, 229.
- (14) Peled, E.; Duvdevani, T.; Aharon, A.; Melman, A. *Electrochem. Solid-State Lett.* **2000**, *3*, 525.
- (15) Scott, K.; Taama, W. M.; Argyropoulos, P. *J. Membr. Sci.* **2000**, *171*, 119.
- (16) Yang, C.; Srinivasan, S.; Arico, A. S.; Creti, P.; Baglio, V.; Antonucci, V. *Electrochem. Solid-State Lett.* **2001**, *4*, A31.
- (17) Kellers, J.; Zhang, W.; Jorissen, L.; Gogel, V. *J. New Mater. Electrochem. Syst.* **2002**, *5*, 97.
- (18) Nunes, S. P.; Ruffmann, B.; Rikowski, E.; Vetter, S.; Richau, K. *J. Membr. Sci.* **2002**, *203*, 215.
- (19) Manea, C.; Mulder, M. *J. Membr. Sci.* **2002**, *206*, 443.
- (20) Kim, J.; Kim, B.; Jung, B. *J. Membr. Sci.* **2002**, *207*, 129.
- (21) Jung, D. H.; Cho, S. Y.; Peck, D. H.; Shin, D. R.; Kim, J. S. *J. Power Sources* **2002**, *106*, 173.
- (22) Shao, Z.-G.; Wang, X.; Hsing, I.-M. *J. Membr. Sci.* **2002**, *210*, 147.
- (23) Heitner-Wirguin, C. *J. Membr. Sci.* **1996**, *120*, 1.
- (24) Kellers, J.; Ullrich, A.; Meier, F.; Haring, Th. *Solid State Ionics* **1999**, *125*, 243.
- (25) Pu, C.; Huang, W.; Ley, K. L.; Smotkin, E. S. *J. Electrochem. Soc.* **1995**, *142*, 119.
- (26) Jia, N.; Lefebvre, M. C.; Halfyard, J.; Qi, Z.; Pickup, P. G. *Electrochem. Solid-State Lett.* **2000**, *3*, 529.
- (27) Michaels, A. S.; Mir, L.; Schneider, N. S. *J. Phys. Chem.* **1965**, *69*, 1447.
- (28) Michaels, A. S.; Miekka, R. G. *J. Phys. Chem.* **1961**, *65*, 1765.
- (29) Michaels, A. S. *Ind. Eng. Chem.* **1965**, *57* (10), 32.
- (30) Jyh-Jeng Shieh, Robert Y. M. Huang. *J. Membr. Sci.*, **1997**, *127*, 185–202.
- (31) Becker, W.; Naake, G. S. *Chem. Eng. Technol.* **2002**, *25*, 364–370.
- (32) Pivovar, B. S.; Wang, Y.; Cussler, E. L. *J. Membr. Sci.* **1999**, *154*, 155–162.
- (33) Zhou, X. Y.; Lvov, S. N.; Fedkin, M.; Allcock, H. R.; Hofmann, M. A.; Chalkova, E. *J. Membr. Sci.* **2002**, *201*, 47–54.
- (34) Cahan, B. D.; Wainright, J. S. *J. Electrochem. Soc.* **1993**, *140*, 185.
- (35) Haufe, S.; Flemming, U. *J. Membr. Sci.* **2001**, *185*, 95–103.
- (36) Miyatake, K.; Oyaizu, K.; Tsuchida, E.; Hay, A. S. *Macromolecules* **2001**, *34*, 2065.
- (37) Colomban, P.; Novak, A. In *Proton Conductors*; Colomban, P., Ed.; Cambridge University Press: Cambridge, England, 1992; pp 46–51.